Journal of Power Sources 189 (2009) 988–993

Contents lists available at ScienceDirect

Journal of Power Sources

journal homepage: www.elsevier.com/locate/jpowsour

Determination of occurrence of anodic excursion peaks by dynamic electrochemical impedance spectroscopy, atomic force microscopy and cyclic voltammetry

K. Darowicki, K. Andrearczyk*

Department of Electrochemistry Corrosion and Materials Engineering, Gdansk University of Technology, 11/12 Narutowicza Street, 80-952 Gdansk, Poland

ARTICLE INFO

Article history:
Received 6 November 2008
Received in revised form 7 January 2009
Accepted 18 January 2009
Available online 14 February 2009

Keywords:
Lead
Anodic layer
Impedance
PbO_2
Anodic excursion peak

ABSTRACT

The compositions of lead anodic layers and structure strongly depends on, additives, concentration of sulfuric acid, and on potential region. A phenomenon of anodic excursion peaks was always in focus of many researches. In this work the behaviour of anodic excursion peak (AEP) in 0.5 M H_2SO_4 solution is widely investigated by dynamic electrochemical impedance spectroscopy (DEIS), atomic force microscopy (AFM) and cyclic voltammetry (CV) methods. The changes of the impedance spectra and AFM images as a function of potential are presented in this paper. It is suggested that the occurrence of anodic excursion peaks cannot be caused by oxidation of bare metal induced by cracking, it can be related to the oxidation of anodic layer to the oxides with higher non-stoichiometric coefficient.

1. Introduction

Although the first accumulator was discovered in 1859, the behaviour of lead in sulfuric acid solution is still a subject of many investigations still some aspects remain unresolved. The behaviour of the positive electrode was studied by many authors [1–9]. Also the influence of H_2SO_4 on phase composition, mechanism of the processes and electrochemical activity of the PbO_2 was widely investigated [1,2]. Takehara [3] studied dissolution and precipitation reactions on lead sulfate and mechanism of charge/discharge on positive (PbO_2) electrodes. Also the influence of additives; Sn, Ca, and Sb (as an alloy additives) [4–7,9] and Co ions (as an electrolyte additive) were examined [8]. The behaviour of anodic layer was examined especially by cyclic voltammetry (CV) [2,10–12], electrochemical impedance spectroscopy (EIS) [5,13,14], atomic force microscopy (AFM) [9,15,16], scanning electron microscopy (SEM) [1–3,13] and X-ray diffraction (XRD) [1,2,13] methods. Schiota et al. who observed the in situ changes of morphology of a lead dioxide electrode during the oxidation–reduction processes by AFM measurement, emphasized the AFM method as "a new analysis technique for the detailed understanding of the reaction processes in lead-acid batteries, because the AFM can make in situ observation of the electrode surface morphology and its change" [16].

Although the behaviour of lead in sulfuric acid was examined intensively, the reason for the occurrence of anodic excursion peaks (AEPs) has not been unequivocally explained. AEP is a rise of anodic current during the cathodic sweep polarization. The occurrence of AEPs was in the area of interest of many authors, therefore different opinions about that phenomenon were proposed. In early 1980s, Sunderland [10] suggested that the occurrence of AEPs was related to reaction of oxidation water by PbOOH species (2), which formed during the first step of reduction of lead dioxide (1):

$$PbO_2 + H^+ + e = PbOOH \text{ (first step in reduction of lead dioxide)} \quad (1)$$

$$PbOOH + H_2O \rightarrow PbOOH\text{–}OH + H^+ + e \text{ (rate determinating step of oxidation water to oxygen and protons-possible reason for anodic excursion peak occurrence)} \quad (2)$$

$$PbOOH + H^+ + e = PbO + H_2O \text{ (second step in reduction of lead dioxide)} \quad (3a)$$

* Corresponding author. Tel.: +48 58 347 10 92; fax: +48 58 347 10 92.
E-mail addresses: corolla@chem.pg.gda.pl, bonzai@wp.pl (K. Andrearczyk).

0378-7753/$ – see front matter © 2009 Published by Elsevier B.V.
doi:10.1016/j.jpowsour.2009.01.039

Nomenclature

AEP	anodic excursion peak
AFM	atomic force microscopy
DEIS	dynamic electrochemical impedance spectroscopy
CV	cyclic voltammetry
EIS	electrochemical impedance spectroscopy
SEM	scanning electron microscopy
XRD	X-ray diffraction

Or $PbOOH + H^+ + e$

$\rightarrow Pb(OH)_2$ (second step in reduction of lead dioxide [17]) (3b)

$$Pb(OH)_2 + H_2SO_4 \rightarrow PbSO_4 + H_2O \quad (4)$$

(Lead dioxide comprise crystal PbO_2 and amorphous zones $PbO(OH)_2$ which were studied intensively by Pavlov [1,2,12,20]).

The opinion mentioned above is in accordance with investigations performed by Fletcher and Matthews [18], who noticed that during the anodic reaction no photocurrent was recorded, which might be due to the Pb(III) species.

Different explanation was proposed by Czerwiński et al. [11], who suggested that the anodic reaction was due to the oxidation of metallic lead. During reduction of PbO_2 to $PbSO_4$ the molar volume increases, leading to stresses and later to cracking, which exposes the metal allowing the immediate reaction of oxidation on the surface of $PbSO_4$. Metikos-Hukovic et al. [14] and Laitinen et al. [19] described the anodic anomalies as oxidation of lead and/or other not fully oxidated species.

Since the differences between the opinions regarding AEP phenomenon have not been yet resolved, the authors of this paper decided to take up detailed investigations, using latest methods, in order to elucidate the causes of AEPs occurrence.

2. Experiments

The investigations on lead were performed in three-electrode system in 0.5 M H_2SO_4. The working electrode was lead rod (99.9999 purity, 5 mm diameter, Alfa Aesar GmbH & Co. KG), grinded with 800 grade emery paper and rinsed with 5% HNO_3 to remove monoxides and with three-distillated water. The reference electrode in voltammetric and impedance measurements was calomel one (SCE), counter electrode was a platinum sheet. All potentials mentioned in this paper refer to SCE electrode.

Linear sweep voltammetry (LSV) measurements were performed with different sweep rate: 1, 5, 25, 50, 100, and 200 mV s^{-1}, in sulfuric acid 0.5 M, and within different potential regions on Princeton Parstat 2263.

In potentiodynamic method (DEIS) ac perturbation signal, contained sinusoids from the frequency range: 0.7 Hz to 4.5 kHz. It was generated by National Instruments PXI 6120 card while, for dc perturbation, 33120 Agilent generator was used. Furthermore KGLstat v.4.1. (potentiostat) was used in order to apply the signals on the investigated system. Acquisition, analysis and decomposition of signals were performed in Labview 7.1.

For AFM measurements a microscope of NT-MDT Company was used. The lead sample – working electrode – was put into an electrochemical cell where the reference electrode was a silver rod, and the platinum plate was a counter one. The surface was scanned with silicon probe CSG10. The probe parameters were: chip size: 3.6 × 1.6 × 0.4 mm, reflective side: Au, cantilever number: 1 rectangular, tip height: 10–15 μm, tip cone angle ≤22°, tip curvature radius: 10 nm. The scan point size was 256 × 256 and the scan velocity: 25.44 μm s^{-1}. Firstly 2 cycles were performed from −0.8 to 1.8 vs. SCE, then at four different potentials (15 min per each one) in anodic excursion peak area, the topography of the surface was done.

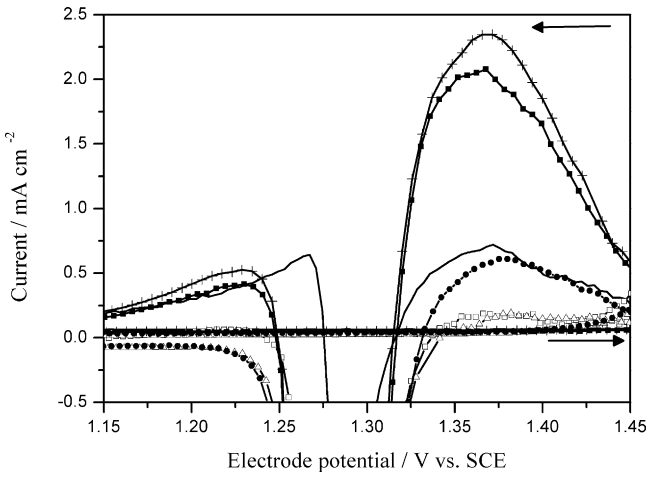

Fig. 1. Voltammograms obtained at different initial potentials to negative ones at 1 mV s^{-1} where: (—) E_1 = 0 V; (□) E_2 = −0.2 V; (△) E_5 = (0.4 V; (●) E_6 = (0.5 V; (■) E_9 = (0.8 V; (+) E_{11} = (1.0 V.

3. Results

In order to estimate the potential at which AEPs occur, chronovoltamperometrical experiment was conducted to determine the influence of initial potential on AEPs occurrence. For the first series of sweeps the initial potential was increased (starting from 0 V, with 0.1 V step) towards negative ones, while the final potential – 1.8 V (oxygen evolution) – was kept constant. In Fig. 1a part of obtained voltammogram at sweep rate 1 mV s^{-1} is shown.

Depending on the initial potential of scanning, different AEPs values are obtained, if the potential is within −0.4 to 0 V range, AEPs are weakly formed. For initial potentials from −0.5 to −1.0 V formation and increase of AEPs values can be observed (see Fig. 1). The highest values of currents, accompanying the AEPs, were obtained for −1.0 V potential.

For the next series of sweeps the initial potential was increased (starting from 0 V, with 0.1 V step) towards positive ones, while again the final potential – 1.8 V (oxygen evolution) – was kept constant. The obtained voltammogram at sweep rate 1 mV s^{-1} is shown in Fig. 2.

It can be observed that with the increase of initial potential AEPs decay. At 0.4 V the formation of "G" peak begins at the expense of the decaying AEPs. With the increase of initial potentials the "G" peak decreases and moves to the left. When polarizing the sample towards negative potentials, the "G" peak does not occur (see Fig. 1).

Taking the obtained voltammograms into consideration, it should be assumed that initial potential has a significant influence on AEPs occurrence. In particular the reaction of $PbSO_4$ reduction to Pb effects the formation of AEPs.

In order to understand the effect of oxygen evolution on AEPs formation, while preserving the area in which the reduction to Pb occurs, the investigated system was subjected to another chronovoltamperometrical experiment. Initial potential was set to −1.0 V (value necessary for visible formation of AEPs) and final potential was set to 1.6, 1.8, 2.0 and 2.2 V (Fig. 3a–d, respectively).

For the final potential equal to 1.6 V the oxygen evolution did not proceed, therefore "D" peak, responsible for reduction of PbO_2 to $PbSO_4$ was not observed. AEP also did not occur (see Fig. 3a).

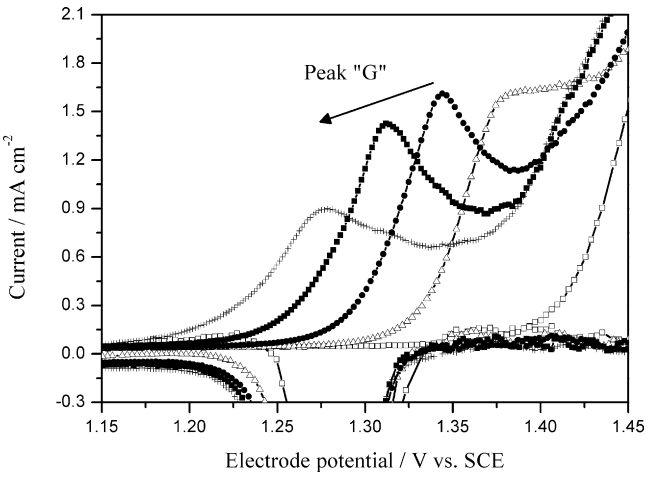

Fig. 2. Voltammograms obtained at different initial potentials to positive ones, at 1 mV s^{-1}, where: (—) E_1 = 0 V; (□) E_2 = 0.2 V; (△) E_5 = 0.4 V; (●) E_7 = 0.6 V; (■) E_9 = 0.8 V; (+) E_{11} = 1.0 V.

For the final potential equal to 1.8 V (see Fig. 3b) the current accompanying oxygen evolution, as well as the positive hysteresis and "D" and AEP peaks increase in each cycle.

For the final potential equal to 2.0 V (see Fig. 3c) the current accompanying oxygen evolution, as well as "D" and AEP peaks are better formed in each cycle. The positive hysteresis does not occur, since this potential is sufficient for PbO_2 formation.

It is worth remarking that the higher the oxygen evolution current is, the higher the values of AEP and "D" peaks are.

In the voltammogram, for which the final potential is equal to 2.2 V (see Fig. 3d) one can observe the decay of AEPs with each cycle, despite the highest oxygen evolution current and slight increase of "D" peak.

Based on the obtained results it can be concluded that oxygen evolution also has a significant effect on AEPs occurrence.

In the next stage of experiments, the influence of the rate of potential changes on AEP phenomenon was investigated. The system was examined for different rate values: 5, 25, 50, 100, and 200 mV s^{-1} and in constant potential range 0.8–2.1 V for 20 cycles. For 5 mV s^{-1} the highest AEPs values were observed (see Fig. 4). For 100 and 200 mV s^{-1} the peaks did not occur.

In Fig. 4 it can be observed that in successive cycles the AEPs decay. Additionally, during anodic scan one can observe the formation of "G" peak accompanying the decay of AEPs.

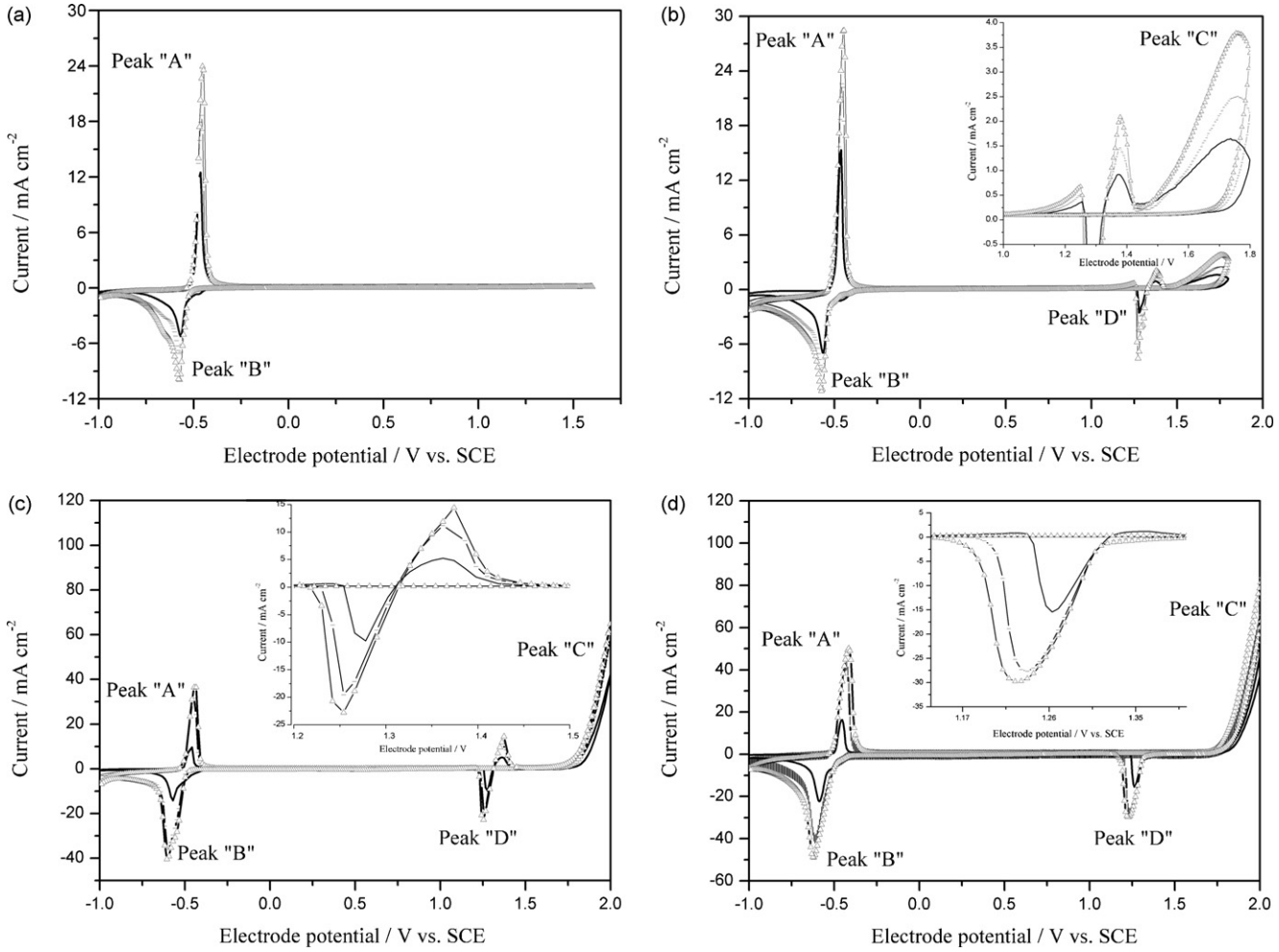

Fig. 3. (a) Voltammograms obtained at sweep rate 5 mV s^{-1}, the potential range from −1.0 to 1.6 V, where: (—) 1st cycle; (□) 5th cycle; (△) 10th cycle. (b) Voltammograms obtained at sweep rate 5 mV s^{-1}, the potential range from −1.0 to 1.8 V, where: (—) 1st cycle; (□) 5th cycle; (△) 10th cycle. (c) Voltammograms obtained at sweep rate 5 mV s^{-1}, the potential range from −1.0 to 2.0 V, where: (—) 1st cycle; (□) 5th cycle; (△) 10th cycle. (d) Voltammograms obtained at sweep rate 5 mV s^{-1}, the potential range from −1.0 to 2.2 V, where; (—) 1st cycle; (□) 5th cycle; (△) 10th cycle.

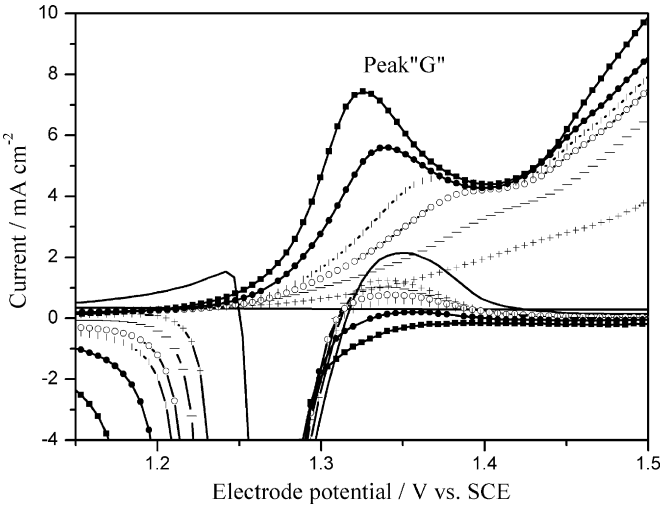

Fig. 4. Voltammograms obtained at 5 mV s^{-1}, where: (—) 1st cycle; (+) 2nd cycle; (□) 3rd cycle; (○) 4th cycle; (|) 5th cycle; (●) 8th cycle; (■) 20th cycle.

Based on the experiments results one can name three factor that influence the occurrence of AEPs: the initial potential (area of $PbSO_4$ to Pb reduction), the final potential (area of oxygen evolution) and the rate of potential changes.

Knowing the dependence of AEPs formation on potential change rate (the lower rate is the better AEPs are formed), as well as the range of potential, the sample was investigated in details using DEIS. The use of potentiodynamic method allowed to obtain the impedance spectra as a function of changing potential. Presented in Fig. 5 is the area in which "the AEP area" and "D" peak, responsible for PbO_2 do $PbSO_4$ reduction, can be observed.

The visible minimum of the spectrogram is responsible for PbO_2 do $PbSO_4$ reduction ("D" peak). The expansion of impedance spectra after passing the minimum is related to the $PbSO_4$ layer. Impedance spectra change monotonously in the whole potential range. Based on this monotonicity it can be stated that cracking is not the cause of AEPs occurrence.

In order to reliably prove that AEPs occurrence is not accompanied by any stresses and cracking of anodic layer, the topography of the anodic layer's surface was investigated using AFM. It enabled acquisition of topography changes of the same region for various potentials. The sequences of topography examination, as well as the direction of potential changes, were determined by the fact that AEPs are formed during cathodic polarization. The AFM images were taken at potentials: 1.35, 1.27, 1.22 and 1.17 V, which were from the range of AEPs occurrence (see Fig. 6). The topographical images (Fig. 7a–d) were obtained after 15 min of lead polarization at each potential. Despite small potential changes the obtained topographical images (Fig. 7a–d) differ significantly. In Fig. 7a one can see a PbO_2 layer composed of globular PbO_2 particles with $PbSO_4$ crystal preserved in right bottom corner. When potential decreases PbO_2 decays (see Fig. 7b–d) while $PbSO_4$ crystals expand significantly (see Fig. 7c and d). Additionally, for E = 1.17 V (Fig. 7d), one can see a privileged spot for crystals formation in the scratch on the sample's surface that was done while grinding emery paper. No cracking caused by PbO_2 to $PbSO_4$ reduction were observed.

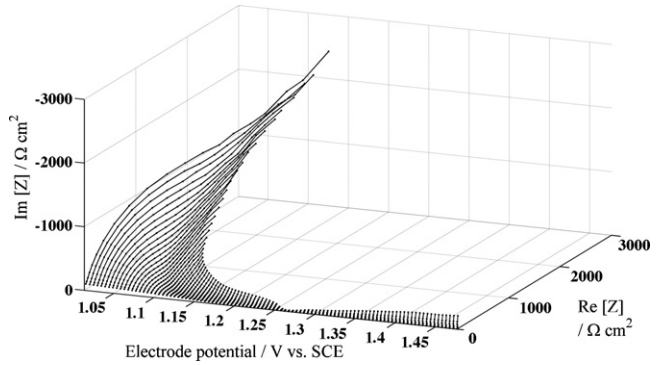

Fig. 5. Spectogram obtained in anodic excursion peak area.

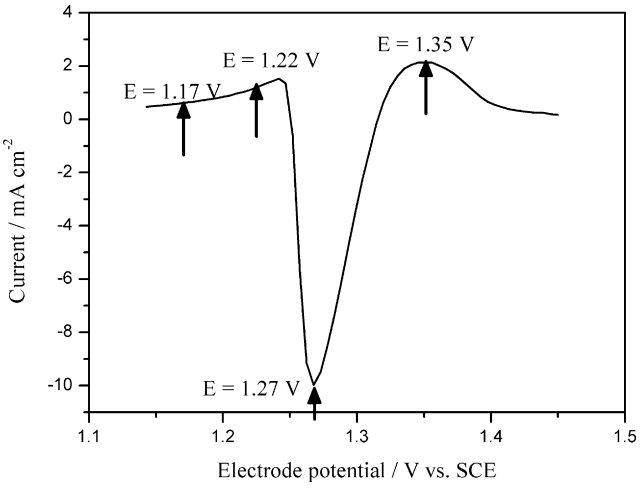

Fig. 6. Potentials for which the surface of anodic layer was investigated using AMF.

4. Discussion

The initial and final potential influences the structure of the anodic layer. The reason of successive AEPs values increase along with shifting initial potentials towards negative ones is that the area of $PbSO_4$ to Pb reduction lies in the range between −0.5 and −1.0 V. The highest values of currents accompanying AEPs were obtained for −1.0 V, that is for the potential more negative than the potential of $PbSO_4$ reduction (see Fig. 1).

While shifting initial potentials towards positive ones AEPs decay. It is worth underlying that with the decay of AEPs one can observe the formation of "G" peak, which can be related for α-PbO_2 forming [8,13,18].

α-PbO_2 oxide is the result of closer packing of tet-PbO via solid state mechanism. "G" peak occurs for potential equal 0.4 V (see Fig. 2). For polarizing the sample towards negative potentials, "G" peak cannot be observed (see Fig. 1).

It can be related to the fact that the anodic layer is reduced to an oxide with smaller "n" coefficient. Therefore "G" peak does not occur.

As it can be seen in Fig. 3a–d, AEP forming is significantly influenced by final potential and oxygen evolution process. Preserving the potential area, in which the reduction of $PbSO_4$ to Pb proceeds, leads to obtaining anodic peaks. They increase alongside with oxygen evolution and, as the result, with consecutive cycles (see Fig. 3b and c). The oxygen evolution current is directly proportional to "D" peak, which is responsible for PbO_2 to $PbSO_4$ reduction. However, for very high values of oxygen evolution current (ca 35 mA) one does not observe significant changes in "D" peak value—the increase of "D" peak value from Fig. 3d is imperceptible compared to the one in Fig. 3c. During oxygen evolution the enrichment of anodic layer in oxygen supervenes resulting in higher "n" coefficient of anodic layer under PbO_2 oxide [20]. The AEPs decay in successive cycles (Fig. 3d) for the increase in current related to oxygen evolution there is an increase in "n" coefficient in anodic layer. Based on above facts one can make a hypothesis that the reaction that

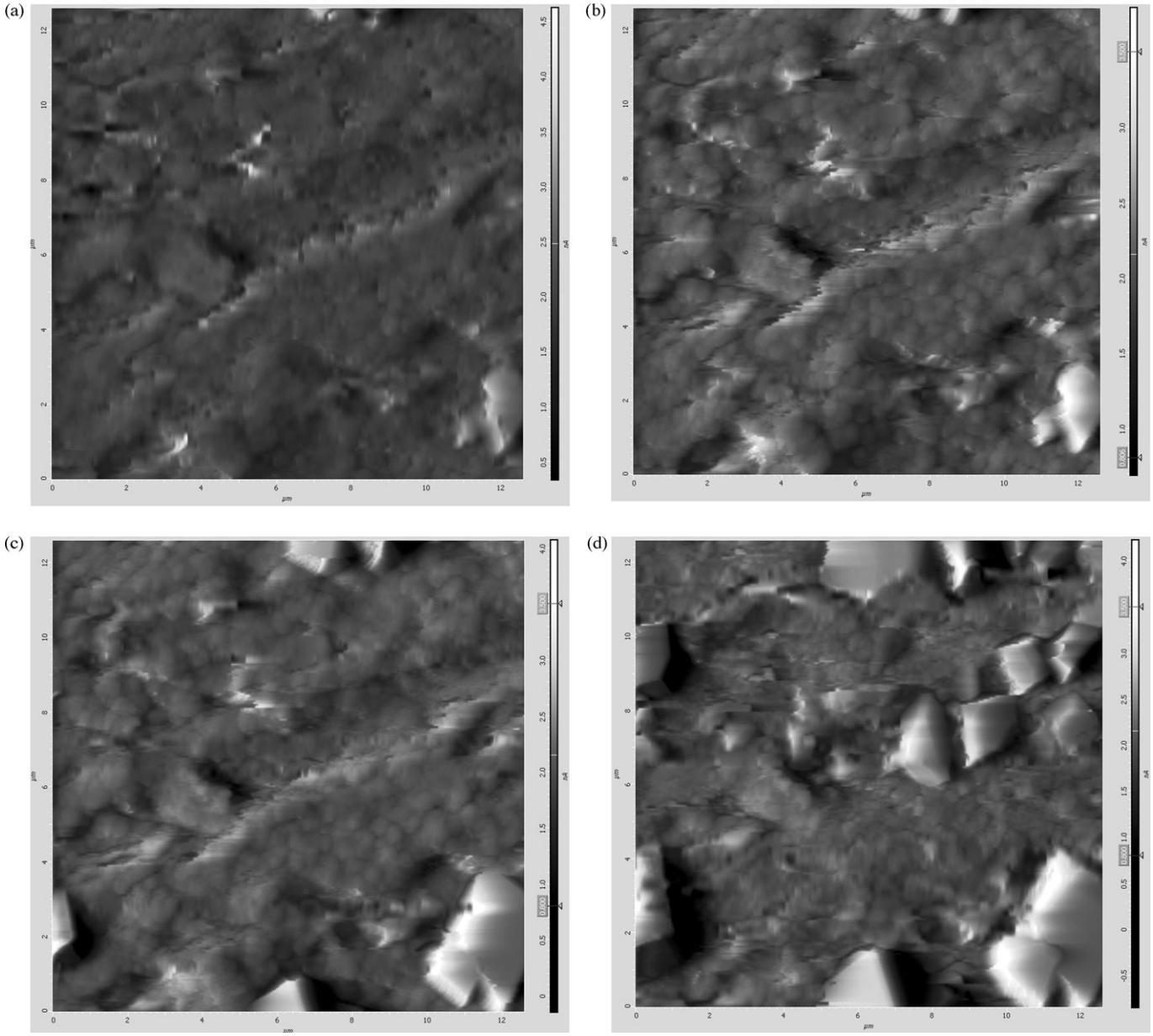

Fig. 7. (a) Topography of an anodic layer formed after 15 min polarization at $E = 1.35$ V. (b) Topography of an anodic layer formed after 15 min polarization at $E = 1.27$ V. (c) Topography of an anodic layer formed after 15 min polarization at $E = 1.22$ V. (d) Topography of an anodic layer formed after 15 min polarization at $E = 1.17$ V.

accompanies AEPs is related to the increase of "n" coefficient in non-stoichiometric oxide layer. In case of higher "n" values (Fig. 3d) for high oxygen evolution current the AEP peak do not occur. In case of lower current values while oxide layer enrichment, AEP increases and can cause the increase of "n" coefficient in successive cycles (see Fig. 3b and c). The structure of the anodic layer influences the AEP's occurrence.

By measuring the impedance spectra changes with potential (DEIS method) the spectrogram in AEPs occurrence area was obtained. The spectra change fluently and monotonously, which should not be observed in the case of cracking (see Fig. 5). Visible impedance increase after passing the minimum (PbO_2 to $PbSO_4$ reduction process) is responsible for forming $PbSO_4$ product, which is not an electronic conductor [3].

The reduction process takes place in amorphous layer in accordance with a proton-electron mechanism [17,21].

"Obtained changing images of the topography of the same area confirm spectrogram obtained by DEIS: cracking, which accompanies the reaction described above, are not present on the surface for any potential". In the photographs one can see either fluent covering of the surface with new $PbSO_4$ crystals or fluent expansion of existing ones (see Fig. 7a–d). The micrographs confirm well the conclusion based on DEIS data that no cracks are formed.

Considering that cracking does not occur on the surface the hypothesis presented by Czerwiński et al. [11] appears to be incorrect. Thus the cause of AEPs occurrence is not the result of bare metal oxidation induced by cracking that accompanies stresses during PbO_2 to $PbSO_4$ reduction. On the other hand, taking into consideration the electrochemical character of AEPs (confirmed with the use of voltammetry), one can assume that the theory of AEPs forming as the result of water oxidation to PbOOH proposed by Sunderland [10] can be correct. The consecution of reaction described by Sunderland can be the enrichment of the layer in oxide that has higher "n" coefficient, which was confirmed with voltammetry experiments.

5. Conclusions

The occurrence of AEPs cannot be related to the oxidation of bare metal induced by cracking caused by increased molar volume during the reduction of PbO_2 to $PbSO_4$, as proposed by Czerwiński et al. in [11]. It is proved by the fluent change of impedance spectra and the topographical images vs. the potential. The cracking occurs only when the whole exposed surface is coated with PbO_2, while it was shown that AEPs occur within the first 20 cycles when the layer is not entirely created. Based on the obtained results authors state that cracking is not the cause of anodic excursion peaks occurrence.

References

[1] D. Pavlov, A. Kirchev, M. Stoychera, B. Monahov, J. Power Sources 137 (2004) 288–308.
[2] B. Monahov, D. Pavlov, A. Kirchev, S. Vasilev, J. Power Sources 113 (2003) 281–292.
[3] Z. Takehara, J. Power Sources 85 (2000) 29–37.
[4] K. Sawai, Y. Tsuboi, Y. Okada, M. Shiomi, S. Osumi, J. Power Sources 179 (2008) 799–807.
[5] M. Metikos-Hukovic, R. Babic, S. Brinic, J. Power Sources 157 (2006) 563–570.
[6] N. Bui, P. Mattesco, P. Simon, N. Pebere, J. Power Sources 73 (1998) 30–35.
[7] N. Bui, P. Mattesco, P. Simon, J. Steinmetz, E. Rocca, J. Power Sources 67 (1997) 61–67.
[8] T. Nguyen, A. Atrens, J. Appl. Electrochem. 38 (2008) 569–577.
[9] M. Shiota, Y. Yamaguchi, Y. Nakayama, N. Hirai, S. Hara, In situ EC-AFM observation of antimony effect for lead dioxide electrode, J. Power Sources 113 (2003) 277–280.
[10] J. Sunderland, J. Electroanal. Chem. 71 (1976) 341–345.
[11] A. Czerwiński, M. Zelazowska, M. Grden, K. Kuc, J.D. Milewski, A. Nowacki, G. Wojcik, M. Kopczyk, J. Power Sources 85 (2000) 49–55.
[12] D. Pavlov, Z. Dinev, J. Electrochem. Soc. 127 (1980) 855–863.
[13] D. Zhou, L. Gao, Electrochim. Acta 53 (2007) 2060–2064.
[14] M. Metikos-Hukovic, R. Babic, S. Brinic, J. Power Sources 64 (1997) 13–19.
[15] K. Uosaki, K. Konishi, M. Koinuma, Langmuir 13 (1997) 3557–3562.
[16] M. Shiota, Y. Yamaguchi, Y. Nakayama, K. Adachi, S. Taniguchi, N. Hirai, S. Hara, J. Power Sources 95 (2001) 203–208.
[17] R. Fitas, N. Chelali, L. Zerroual, B. Djellouli, Solid State Ion. 127 (2000) 49–54.
[18] S. Fletcher, D.B. Matthews, J. Electroanal. Chem. 126 (1981) 131.
[19] T. Laitinen, K. Salmi, G. Sundholm, B. Monahov, D. Pavlov, Electrochim. Acta 36 (1991) 605–614.
[20] D. Pavlov, B. Monahov, J. Electrochem. Soc. 143 (1996) 3616–3629.
[21] A. Kirchev, A. Delaille, M. Perrin, E. Lemaire, F. Mattera, J. Power Sources 170 (2007) 495–512.